Lateral Dynamics and Stability Analysis of a Gas Compressor Supported by Hybrid and Active Lubricated Multirecess Journal Bearing

Ilmar F. Santos
ifs@mek.dtu.dk
Technical University of Denmark - DTU
Department of Engineering
2800, Lyngby. Denmark

Flávio Y. Watanabe
Member, ABCM
fywatana@unimep.br
Methodist University of Piracicaba - UNIMEP
18450-000 Sta. Bárbara d'Oeste, SP. Brazil

Fluid film forces are generated in multirecess journal bearings by two types of lubrication mechanism: the hydrostatic lubrication in the bearing recesses and hydrodynamic lubrication in the bearing lands, when operating in rotation. The combination of both lubrication mechanism leads to hybrid journal bearings (HJB). When part of hydrostatic pressure is also dynamically modified by means of hydraulic control systems, one refers to the active lubrication, resulting in the active hybrid journal bearing (AHJB). The AHJB is mathematically modeled based on the Reynolds' equations in land regions and a set of modified continuity equations for the lubricant flow in the bearing recesses, coupled to equations describing pressure and flow in the servovalves. The solution of such a set o equations allows the determination of fluid film stiffness and damping coefficients of the hybrid and/or active lubricated bearing. Such coefficients are a function of design and operational parameters, characterized by the Sommerfeld number as well by the gains of the feedback control system. The main contribution of the present theoretical work is to analyze the stability characteristics of a flexible rotor-bearing system by using passively and actively lubricated hybrid journal bearing. The dynamic of a flexible rotor is modeled by using finite element method and, after coupling the bearing dynamic coefficients to the rotor model, the feedback control law is defined and a suitable set of control gains is calculated for the active lubrication, leading to a rotor with a wider and more safety operational frequency range.
Keywords*: Hybrid bearing, active lubrication, vibration control, stability*

Introduction

Aiming for the vibration reduction in rotating machines to safety levels, new mechanisms for dissipating vibration energy have been developed, like seal dampers (Vance and Li, 1996), squeeze-film dampers (San Andrés and Lubell, 1998), hybrid squeeze-film dampers (El-Shafei and Halthout, 1995), hydraulic active chamber systems (Ulbrich and Althauss, 1989; Althaus *et al*., 1993; Santos, 1995), variable impedance hydrodynamic journal bearings (Goodwin *et al*., 1989), actively lubricated tilting-pad bearings (Santos, 1994; Santos and Russo, 1998; Santos and Nicoletti, 1999; Santos and Scalabrin, 2003), active-controlled hydrostatic bearings (Bently *et al*., 2000), magnetized journal bearings lubricated with Ferro fluids (Osman *et al*., 2001), and actively lubricated hybrid multirecess journal bearings (Santos and Watanabe, 2003 and 2004).

Recent theoretical and experimental investigations related to active lubrication have been shown the feasibility of attenuating rotor vibrations in test rigs with rigid rotors (Santos, 1994; Santos and Russo, 1998; Santos and Nicoletti, 2001; Santos and Scalabrin, 2003; Santos *et al*., 2001). The use of active lubrication in tilting-pad journal bearings (TPJB) has the strong advantage of resulting in bearings with negligible fluid film cross-coupling effects between orthogonal directions. However, this kind of active strategy can also be applied to hydrostatic or hybrid bearings (Bently *et al*., 2000; Santos and Watanabe, 2003 and 2004), and to multi-lobed bearings (Santos *et al*., 2001).

The main contribution of the present theoretical work is to analyze the feasibility of applying multirecess journal bearings under hybrid and active lubrication regimes to a flexible rotor (industrial gas compressor) with the aim of attenuating rotor lateral vibrations. In the hybrid lubrication case, the hydrostatic pressure in all four recesses is statically modified, allowing an adjustment of the bearing stiffness. In the active lubrication case, the pressure and flow into opposed pair of recesses are dynamically modified with help of servo-hydraulic control. It results in a significant modification of fluid film forces and, consequently, in an active modification of bearing stiffness and damping coefficients. The mathematical model of hybrid journal bearings presented by Ghosh *et al*. (1989) and Guha *et al*. (1989) is extended by including the dynamics of servo control system, as presented by Santos and Russo (1998). A multirecess hybrid journal bearing with active lubrication is termed active hybrid journal bearing (AHJB). The AHJB static and dynamic coefficients are numerically calculated by solving the complete set of continuity equation in recesses regions and Reynolds' Equation in land regions, as a function of Sommerfeld number, perturbation frequency, servovalve dynamic characteristics and feedback control gains. These bearing coefficients, under hybrid and active lubrication regimes, are employed to analyze stability and feasibility of lateral vibration reduction in a gas compressor. The lateral dynamics of the gas compressor is modeled by using finite elements technique. By applying multirecess journal bearings under hybrid and active lubrication regimes to flexible rotor a significant reduction of lateral vibrations at critical speeds and a wider and more safety operational range are achieved.

Nomenclature

a = *circumferential land width, m*
$B_{\varepsilon\varepsilon}, B_{\varphi\varphi}, B_{XX}, B_{YY}$ = *direct damping coefficients, Ns/m*
$B_{\varepsilon\varphi}, B_{\varphi\varepsilon}, B_{XY}, B_{YX}$ = *cross coupling damping coefficients, Ns/m*
b = *axial land width, m*
c = *radial clearance, m*
D = *bearing diameter, m*

Presented at XI DINAME – International Symposium on Dynamic Problems of Mechanics, February 28th - March 4th, 2005, Ouro Preto. MG. Brazil.
Paper accepted: June, 2005. Technical Editors: J.R.F. Arruda and D.A. Rade.

d = *journal diameter, m*
e = *journal eccentricity, m*
f_r = *rotation frequency, Hz*
$g_{1X}, g_{2X}, g_{1Y}, g_{2Y}$ = *direct gain coefficients, V/m*
$g_{3X}, g_{4X}, g_{3Y}, g_{4Y}$ = *cross-coupling gain coefficients, Vs/m*
$\underline{h}$ = *fluid film thickness, m*
$\underline{h}_l^{(n)}$ = *film thickness between n-th and (n+1)-th recesses*
$\boldsymbol{h}_r$ = *film thickness vector at the center recesses*
K_{PQ} = *servovalve flow-pressure coefficient, m^3/sPa*
K_v = *servovalve gain, m^3/sV*
$K_{\varepsilon\varepsilon}, K_{\varphi\varphi}, K_{XX}, K_{YY}$ = *direct stiffness coefficients, N/m*
$K_{\varepsilon\varphi}, K_{\varphi\varepsilon}, K_{XY}, K_{YX}$ = *cross coupling stiffness coefficients, N/m*
L = *bearing length, m*
L_e = *effective recess length (L_e =L-a), m*
l_a = *axial recess length, m*
l_b = *circumferential recess length, m*
P = *fluid film pressure, Pa*
P_L = *servovalve load pressure, Pa*
P_r = *bearing recess pressure, Pa*
P_S = *servovalve supply pressure, Pa*
P_{S0} = *bearing steady state supply pressure, Pa*
$\underline{\boldsymbol{p}}_r$ = *recess pressure vector*
$\boldsymbol{Q}_r$ = *recess flow matrix*
$\overline{\boldsymbol{q}}_S$ = *fluid flow vector injected into the recesses*
R = *bearing radius, m*
r = *journal radius, m*
$\boldsymbol{T}$ = *coordinate transformation matrix*
t = *time, s*
t_r = *recess depth, m*
U = *servovalve input voltage, V*
$\overline{\boldsymbol{V}}_e$ = *effective recess volume matrix*
XYZ = inertial coordinate system
xyz = local coordinate system

Greek Symbols

Δe = *journal dynamic displacement, m*
$\Delta \dot{e}$ = *journal velocity, m/s*
$\Delta P_S^{(n)}$ = *dynamic supply pressure in n-th recess, Pa*
δ_C = *capillary parameter, dimensionless*
ε = *journal eccentricity ratio, dimensionless*
ζ_v = *servovalve damping factor*
Θ = *recess squeeze parameter, dimensionless*
θ = *angular coordinate, rad*
κ = *fluid compressibility parameter, Pa^{-1}*
Λ = *angular velocity parameter, dimensionles*
μ = *fluid absolute or dynamic viscosity, Ns/m^2*
Π = *recess compressibility parameter, dimensionless*
ρ = *fluid volumetric density, kg/m^3*
τ = *time, dimensionless*
Φ = *recess velocity parameter, dimensionless*
φ = *attitude angle, rad*
Ψ = *squeeze or perturbation, dimensionless*
Ω = *journal angular velocity, rad/s*
ω = *perturbation frequency, rad/s*
ω_v = *servovalve eigenfrequency, rad/s*

Subscripts

0 relative to static or steady state condition
1,2 relative to dynamic or perturbed conditions
l relative to land region
op relative to operation point
r relative to recess
s relative to supply conditions
v relative to servovalve
X,Y relative to X and Y directions, respectively
ε,φ *relative to* ε *and* φ *directions, respectively*

Superscripts

(*n*) *relative to n-th recess*
w^* *relative to amplitude of generic parameter w*
$\overline{w}$ *relative to dimensionless form of generic parameter w*

Active Hybrid Journal Bearing - AHJB

The AHJB under investigation has four recesses, aligned in pairs in the horizontal (*Y*) and vertical (*X*) directions and numbered as shown in Fig.1a. The conventional passive bearing operation is warranted by fluid injection into the recesses through capillary restrictors, at a constant pressure supply P_{S0}. Additionally, for active dynamic control of the fluid pressure and compensation of cross-coupling effects, the flow is injected into the opposed bearing recesses pairs, each one of them are connected to servo control systems. Electro-hydraulic servovalves, journal displacement and/or velocity transducers and PD (proportional-derivative) feedback controllers, constitute the servo control system. The servovalves are controlled by electrical voltage signals, U_X and U_Y, generated by the combination of journal dynamic displacement and velocity measurement signals in *X* and *Y* directions. The main geometric characteristics of a four recesses hybrid journal bearing, nomenclature and coordinate systems are represented in Fig. 1.

AHJB Mathematical Modeling

The mathematical model of the HJB is obtained basically by using the Reynolds' equation in the land surfaces and the flow continuity equation in the bearing recesses, as presented by Santos and Watanabe (2003). The modeling technique used is the small perturbation method applied to the journal steady state equilibrium position (Lund and Thomsen, 1978, and by Ghosh et al., 1989). Within the bearing radial clearance *c*, the journal static eccentricity and attitude angle are defined by e_0 and φ_0, respectively, and the journal dynamic perturbations are defined by the real part of the harmonic functions given by $e_1^* e^{i\omega t}$ and $\varphi_1^* e^{i\omega t}$, where e_1^* and φ_1^* are the perturbations amplitudes. The resulting dimensionless fluid film thickness $\overline{h} = h/c$ is defined as a function of the dimensionless eccentricity ratio $\varepsilon = e/c$, the attitude angle φ_1^*, the angular coordinate $\theta = x/R$, and the dimensionless time $\tau = \omega t$.

$$\begin{cases} \overline{h} = \overline{h}_0 + \varepsilon_1^* e^{i\tau} \cos\theta + \varepsilon_0 \varphi_1^* e^{i\tau} \sin\theta \\ \overline{h}_0 = 1 + \varepsilon_0 \cos\theta \end{cases} \tag{1}$$

Considering the small perturbation characteristics, the dimensionless fluid film pressure $\overline{P} = P/P_{S0}$ may be described similarly to dimensionless film thickness $\overline{h}$, defined Eq.(1), as follows

$$\overline{P} = \overline{P}_0 + \varepsilon_1^* e^{i\tau} \overline{P}_1 + \varepsilon_0 \varphi_1^* e^{i\tau} \overline{P}_2 \tag{2}$$

where, the index *0* is relative to steady state condition and the indexes *1* and *2* are relative to dynamic or perturbed conditions.

The fluid film behavior in the land surfaces of a finite bearing is described by the three dimensionless Reynolds' equations, given in Eq.(3-5), deduced by using the Navier-Stokes, continuity equations

and Eq.(1-2), considering a isoviscous incompressible fluid, in laminar flow and including the hydrodynamic and squeeze effects.

$$\frac{\partial}{\partial\theta}\left(\bar{h}_0^3\frac{\partial\bar{P}_0}{\partial\theta}\right)+\left(\frac{D}{L}\right)^2\frac{\partial}{\partial\bar{z}}\left(\bar{h}_0^3\frac{\partial\bar{P}_0}{\partial\bar{z}}\right)=\Lambda\frac{\partial\bar{h}_0}{\partial\theta} \tag{3}$$

$$\left.\begin{aligned}\frac{\partial}{\partial\theta}\left(\bar{h}_0^3\frac{\partial\bar{P}_1}{\partial\theta}\right)+\frac{\partial}{\partial\theta}\left(3\bar{h}_0^2\cos\theta\frac{\partial\bar{P}_0}{\partial\theta}\right)+\left(\frac{D}{L}\right)^2\frac{\partial}{\partial\bar{z}}\left(\bar{h}_0^3\frac{\partial\bar{P}_1}{\partial\bar{z}}\right)+\\+\left(\frac{D}{L}\right)^2\frac{\partial}{\partial\bar{z}}\left(3\bar{h}_0^2\cos\theta\frac{\partial\bar{P}_0}{\partial\bar{z}}\right)=-\Lambda\sin\theta+i\Psi\cos\theta\end{aligned}\right\} \tag{4}$$

$$\left.\begin{aligned}\frac{\partial}{\partial\theta}\left(\bar{h}_0^3\frac{\partial\bar{P}_2}{\partial\theta}\right)+\frac{\partial}{\partial\theta}\left(3\bar{h}_0^2\cos\theta\frac{\partial\bar{P}_0}{\partial\theta}\right)+\left(\frac{D}{L}\right)^2\frac{\partial}{\partial\bar{z}}\left(\bar{h}_0^3\frac{\partial\bar{P}_2}{\partial\bar{z}}\right)+\\+\left(\frac{D}{L}\right)^2\frac{\partial}{\partial\bar{z}}\left(3\bar{h}_0^2\cos\theta\frac{\partial\bar{P}_0}{\partial\bar{z}}\right)=\Lambda\cos\theta+i\Psi\sin\theta\end{aligned}\right\} \tag{5}$$

where,

$$\bar{z}=2z/L$$

$$\Lambda=6\mu\Omega/P_{s0}\,(c/R)^2$$

$$\Psi=12\mu\omega/P_{s0}\,(c/R)^2$$

Equations (3-5) are solved by using the *finite difference* method with the boundary condition listed below for *k=0* (steady state condition) and for *k=1,2* (dynamic conditions)

(a) $\bar{P}_0(\theta,\bar{z})=0$, in the regions of cavitations (land surfaces)

(b) $\bar{P}_k=\bar{P}_r^{(n)}$, fluid pressure at the *n-th* recess

(c) $\bar{P}_k(\theta,+1)=\bar{P}_k(\theta,-1)=0$, for symmetry

(d) $\bar{P}_k(\theta,\bar{z})=\bar{P}_k(\theta+2\pi,\bar{z})$, for periodicity

(e) $\frac{\partial\bar{P}_k}{\partial\bar{z}}(\theta,0)=0$, for symmetry

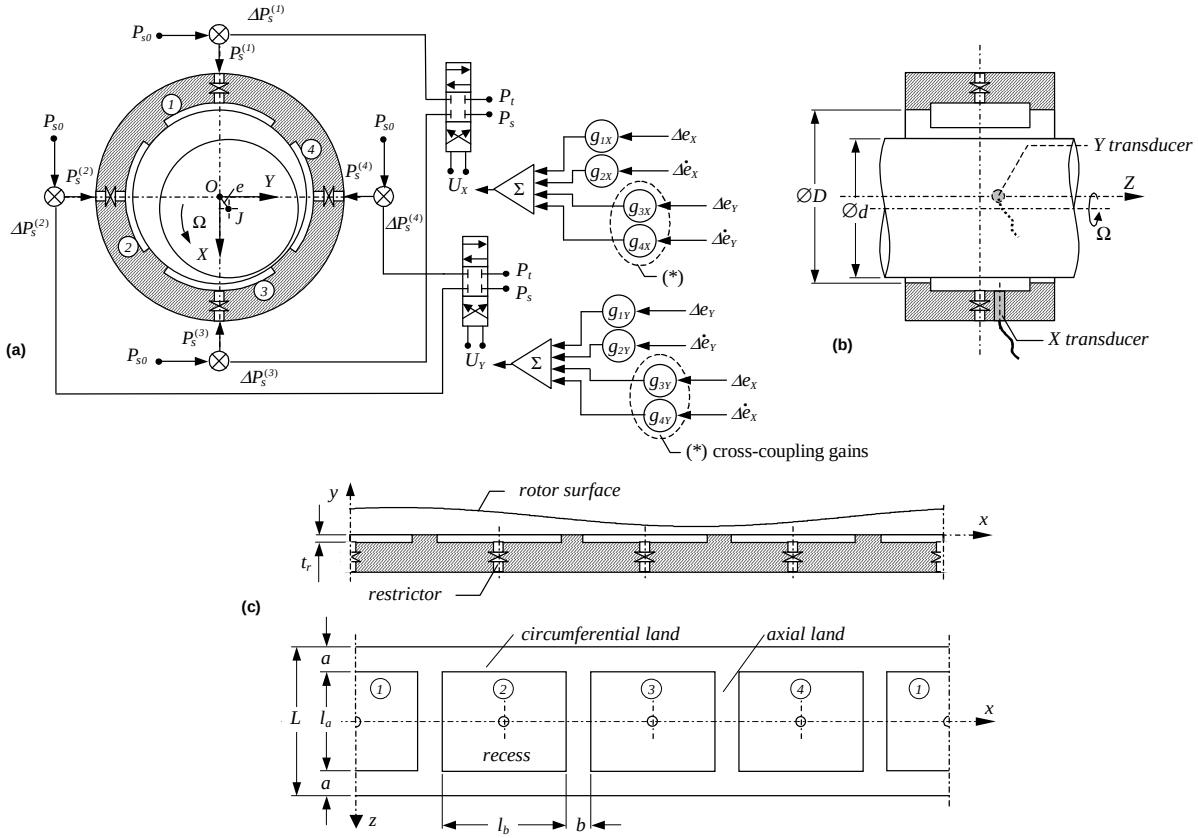

Figure 1. Active Hybrid Journal Bearing – geometric characteristics and operational principle.

The fluid pressures in the recesses are obtained by applying the continuity equation, considering fluid hydrodynamic, hydrostatic, squeeze and compressibility effects. The recess fluid pressures $\bar{P}_r^{(n)}$, in the *n-th* recess, is defined similarly to the fluid film pressure $\bar{P}$ as follows

$$\bar{P}_r^{(n)}=\bar{P}_{r0}^{(n)}+\varepsilon_1^*\bar{P}_{r1}^{(n)}e^{i\tau}+\varepsilon_0\varphi_1^*\bar{P}_{r2}^{(n)}e^{i\tau} \tag{6}$$

Defining the dimensionless flow as follows, $\bar{Q}=12\mu Q/c^3P_{s0}$, and applying the continuity equation to all recesses, results to the following vector equation

$$\bar{\boldsymbol{q}}_s=\bar{\boldsymbol{Q}}_r\bar{\boldsymbol{p}}_r+\Phi\Delta\bar{\boldsymbol{h}}+\Theta\frac{\partial\bar{\boldsymbol{h}}_r}{\partial\tau}+\Pi\bar{\boldsymbol{V}}_e\frac{\partial\bar{\boldsymbol{p}}_r}{\partial\tau} \tag{7}$$

where,

$$\bar{\boldsymbol{q}}_S = \left\{ \bar{Q}_S^{(1)} \quad \bar{Q}_S^{(2)} \quad \bar{Q}_S^{(3)} \quad \bar{Q}_S^{(4)} \right\}$$

$$\bar{\boldsymbol{p}}_r = \left\{ \bar{P}_r^{(1)} \quad \bar{P}_r^{(2)} \quad \bar{P}_r^{(3)} \quad \bar{P}_r^{(4)} \right\}$$

$$\bar{\boldsymbol{h}}_r = \left\{ \bar{h}_r^{(1)} \quad \bar{h}_r^{(2)} \quad \bar{h}_r^{(3)} \quad \bar{h}_r^{(4)} \right\}$$

$$\Delta\bar{\boldsymbol{h}} = \left\{ (\bar{h}_l^{(1)} - \bar{h}_l^{(4)}) \quad (\bar{h}_l^{(2)} - \bar{h}_l^{(1)}) \quad (\bar{h}_l^{(3)} - \bar{h}_l^{(2)}) \quad (\bar{h}_l^{(4)} - \bar{h}_l^{3)}) \right\}$$

$$\Phi = 6\mu U L_e / c^2 P_{s0}$$

$$\Theta = 12\mu\omega D L_e \sin(\pi/4) / c^2 P_{s0}$$

$$\Pi = 12\mu\omega\kappa / c^3$$

The fluid flow $\bar{\boldsymbol{q}}_S$, injected into the bearing recesses, is resultant of the combination of the conventional lubrication supply and the active lubrication systems, whose main components are the servovalves and the type adopted is a two-stage, four-way, critical center or zero-lapped spool electrohydraulic servovalve. In a typical critical center servovalve, the output spool position is proportional to electrical signal applied to torque motor coils. Movement of the spool opens an orifice from the constant supply pressure P_S to one servovalve port and an identical orifice connects the other servovalve port to the return line to reservoir at pressure P_t. In case of having the bearing recess connected to the return line via servovalve port, the value of return pressure P_t has to be adjusted in order to assure a minimum operational pressure in the bearing recess.

The dynamics of the fluid flow through an unloaded servovalve can be described by a second order differential equation (Merrit, 1967). The coefficients of such equation, eigenfrequency ω_v, damping factor ζ_v and gain K_v, are obtained from servovalve manufacturers (Neal, 1974 and Edelmann, 1986). Each servovalve, working in orthogonal directions *X* and *Y*, is described mathematically as a function of the servovalve dynamic coefficients, the unloaded fluid flows Q_{vX} and Q_{vY} and the input electrical voltage signals U_X and U_Y by

$$\begin{cases} \ddot{Q}_{vX} + 2\zeta_v\omega_v\dot{Q}_{vX} + \omega_v^2 Q_{vX} = \omega_v^2 K_v U_X \\ \ddot{Q}_{vY} + 2\zeta_v\omega_v\dot{Q}_{vY} + \omega_v^2 Q_{vY} = \omega_v^2 K_v U_Y \end{cases} \tag{8}$$

The input signals U_X and U_Y are generated as a linear combination of journal displacement and velocity sensors signals, and can be expressed as

$$\begin{cases} U_X = g_{1X}\Delta e_X + g_{2X}\Delta\dot{e}_X + g_{3X}\Delta e_Y + g_{4X}\Delta\dot{e}_Y \\ U_Y = g_{1Y}\Delta e_Y + g_{2Y}\Delta\dot{e}_Y - g_{3Y}\Delta e_X + g_{4Y}\Delta\dot{e}_X \end{cases} \tag{9}$$

where

$$\Delta e_X = e_X^* e^{i\omega t}, \quad \Delta e_Y = e_Y^* e^{i\omega t}$$

$$\Delta\dot{e}_X = i\omega\Delta e_X, \quad \Delta\dot{e}_Y = i\omega\Delta e_Y$$

$$e_X^* = e_1^* \cos\varphi_0 - e_0\varphi_1^* \sin\varphi_0, \quad e_Y^* = e_1^* \sin\varphi_0 + e_0\varphi_1^* \cos\varphi$$

Such a linear combination of journal displacement and velocity signals leads to a PD (proportional-derivative) controller.

As shown in Fig.1a, the servovalve connected to recesses *1* and *3* is responsible for controlling the journal movement in *X* direction, and the other servovalve connected to recesses *2* and *4* is responsible for controlling the journal movement in *Y* direction. For simplicity, the analysis is presented only in *Y* direction.

The unloaded servovalve flow Q_{vY} can be expressed by $Q_{vY} = Q_{vY}^* e^{i(\omega t + \varphi_Y)}$, once it is proportional to the harmonic journal eccentricity. It was assumed that the cross-coupling gains coefficients g_{3Y} and g_{4Y} are proportional to the direct gain coefficients g_{1Y} and g_{2Y}, respectively, and are related as follows: $g_{3Y} = k_g g_{1Y}$ and $g_{4Y} = k_g g_{2Y}$, where k_g is the proportionality constant. The factor k_g only influences the cross stiffness and damping coefficients of the bearing. The inversion of one of the retrofitted displacement signals in Eq.(9) allows the simultaneously reduction of the cross-coupling stiffness coefficients. The crossed retrofitting of linear velocity signals should be avoided, once it contributes to the increase of the whirl frequency ratio (Santos and Watanabe, 2004). One can deduce the Q_{vY} expression from Eq.(8), in dimensionless form

$$\bar{Q}_{vY} = (\varepsilon_Y^* + k_g\varepsilon_X^*) G_Y e^{i(\omega t + \varphi_Y)} \tag{10}$$

where,

$$G_Y = \frac{12\mu\omega_v^2 K_v}{c^2 P_{s0}} \sqrt{\frac{g_{1Y}^2 + \omega^2 g_{2Y}^2}{(\omega_v^2 - \omega^2)^2 + (2\zeta_v\omega_v\omega)^2}}$$

$$\varphi_Y = tg^{-1}\left\{ \frac{-2\zeta_v\omega_v\omega g_{1Y} + \omega(\omega_v^2 - \omega^2) g_{2Y}}{(\omega_v^2 - \omega^2) g_{1Y} + 2\zeta_v\omega_v\omega^2 g_{2Y}} \right\}$$

The active fluid flow injected in *Y* direction Q_Y may be given in the following dimensionless form

$$\bar{Q}_Y = \bar{Q}_{vY} - \bar{K}_{PQ}\bar{P}_{LY} \tag{11}$$

where,

$$K_{PQ} = (\partial Q_Y / \partial P_{LY})_{op}, \quad \bar{K}_{PQ} = 12\mu K_{PQ} / c^3$$

$$\bar{P}_{LY} = P_{LY} / P_{S0} = \bar{P}_S^{(2)} - \bar{P}_S^{(4)} \equiv \Delta\bar{P}_S^{(2)} - \Delta\bar{P}_S^{(4)}$$

The coefficients K_v and K_{PQ} may be experimentally determined as shown by Merrit (1967), and usually are given by servovalve manufacturers. Equation (11) is valid only in a small range of the nominal input signal, usually ±5%. It is important to mention that the gains g_1 and g_2 have to be chosen respecting the linear range of the servovalve dynamics, i.e. the maximum amplitude of the control voltage (servovalve input signal). Mathematically, it means that U_X and U_Y, given by Eq.(9), have to be in the range of ±5% of the nominal voltage . Such an analysis can only be done knowing the vibration amplitudes of the rotor-bearing system.

Generally speaking, as it can be seem in Eq.(9), the bigger the rotor displacements amplitudes e_X^* and e_Y^* are, the smaller the proportional coefficients g_1 and g_2 can be, in order to avoid a large amplitude of control signals U_X and U_Y, and the resulting saturation of servovalve dynamics. Furthermore, the higher the perturbation frequencies ω are, the smaller the derivative gain coefficient g_2 can be, if a controller with derivative part is adopted, once the journal velocities amplitudes are given by ωe_X^* and ωe_Y^*.

Coupling the HJB and servo control system models, results in the complete mathematical model of AHJB (Santos and Watanabe, 2003), and the total fluid flow injected into the bearing recesses are determined as follows

$$\bar{\boldsymbol{q}}_S = \bar{\boldsymbol{q}}_{S0} + (\delta_c\,\bar{\boldsymbol{p}}_{r1} + \bar{\boldsymbol{g}}_{S1})\,\varepsilon_1^* e^{i\tau} + (\delta_c\,\bar{\boldsymbol{p}}_{r2} + \bar{\boldsymbol{g}}_{S2})\,\varepsilon_0\varphi_1^* e^{i\tau} \tag{12}$$

where, $\bar{\boldsymbol{q}}_{s0}$, $\bar{\boldsymbol{p}}_{r1}$ and $\bar{\boldsymbol{p}}_{r2}$ are defined similarly to $\bar{\boldsymbol{q}}_s$ and $\bar{\boldsymbol{p}}_r$, and $\bar{\boldsymbol{g}}_{s1}$ and $\bar{\boldsymbol{g}}_{s2}$ are injection vectors related to the bearing active lubrication system.

Defining the following small amplitude perturbations form for $\bar{\boldsymbol{h}}_r$, $\Delta\bar{\boldsymbol{h}}$ and $\bar{\boldsymbol{Q}}_r$ as follows

$$\begin{cases} \bar{\boldsymbol{h}}_r = \bar{\boldsymbol{h}}_{r0} + \varepsilon_1^* e^{i\tau} cos\,\boldsymbol{\theta}_r + \varepsilon_0 \varphi_1^* e^{i\tau} sin\boldsymbol{\theta}_r \\ \Delta\bar{\boldsymbol{h}} = \Delta\bar{\boldsymbol{h}}_0 + \varepsilon_1 e^{i\tau}\Delta\bar{\boldsymbol{h}}_1 + \varepsilon_0\varphi_1 e^{i\tau}\Delta\bar{\boldsymbol{h}}_2 \\ \bar{\boldsymbol{Q}}_r = \bar{\boldsymbol{Q}}_{r0} + \varepsilon_1 e^{i\tau}\bar{\boldsymbol{Q}}_{r1} + \varepsilon_0\varphi_1 e^{i\tau}\bar{\boldsymbol{Q}}_{r2} \end{cases} \tag{13}$$

where,

$$\bar{\boldsymbol{Q}}_{r1} = \left.\frac{\partial\bar{\boldsymbol{Q}}_r}{\partial\varepsilon}\right|_{\varepsilon=\varepsilon_0} \quad ; \quad \bar{\boldsymbol{Q}}_{r2} = \left.\frac{1}{\varepsilon_0}\frac{\partial\bar{\boldsymbol{Q}}_r}{\partial\varphi}\right|_{\varphi=\varphi_0}$$

Substituting Eq.(12-13) in Eq.(7), and collecting the similar linear terms, results the three following equations

$$\bar{\boldsymbol{q}}_{s0} = \delta_c(\boldsymbol{1}_{4x1} - \bar{\boldsymbol{p}}_{r0}) = \bar{\boldsymbol{Q}}_{r0}\bar{\boldsymbol{p}}_{r0} + \Phi\Delta\bar{\boldsymbol{h}}_0 \tag{14}$$

$$(\bar{\boldsymbol{Q}}_{r0} + \delta_c\boldsymbol{I}_{4x4} + i\Pi\bar{\boldsymbol{V}}_e)\bar{\boldsymbol{p}}_{r1} = -\bar{\boldsymbol{Q}}_{r1}\bar{\boldsymbol{p}}_{r0} - \Phi\Delta\bar{\boldsymbol{h}}_1 - i\Theta cos\,\boldsymbol{\theta}_r + \bar{\boldsymbol{g}}_{s1} \tag{15}$$

$$(\bar{\boldsymbol{Q}}_{r0} + \delta_c\boldsymbol{I}_{4x4} + i\Pi\bar{\boldsymbol{V}}_e)\bar{\boldsymbol{p}}_{r2} = -\bar{\boldsymbol{Q}}_{r2}\bar{\boldsymbol{p}}_{r2} - \Phi\Delta\bar{\boldsymbol{h}}_2 - i\Theta cos\,\boldsymbol{\theta}_r + \bar{\boldsymbol{g}}_{s2} \tag{16}$$

The steady state recess pressure vector $\bar{\boldsymbol{p}}_{r0}$ is obtained solving Eq.(14), and the dynamic recess pressures $\bar{\boldsymbol{p}}_{r1}$ and $\bar{\boldsymbol{p}}_{r2}$ vectors are obtained by solving Eq.(15) and Eq.(16), respectively.

AHJB Dynamic Coefficients

The stiffness and damping coefficients of the AHJB are determined by considering the dynamic restoring forces due to small amplitude perturbed film pressure $\varepsilon_1^* e^{i\omega t} P_1$ and $\varepsilon_0\varphi_1^* e^{i\omega t} P_2$ around the steady state journal equilibrium position, as presented by Ghosh et al. (1989). Considering the perturbed film pressure $\varepsilon_1^* e^{i\omega t} P_1$, the restoring forces along ε_0 and φ_0 directions, denoted by $W_{1\varepsilon}$ and $W_{1\varphi}$, respectively, also can be written as a function of linearized stiffness and damping coefficients. Defining the dimensionless force $\overline{W}_1 = W_1 / LDP_{s0}\varepsilon_1^*$ and the perturbation frequency ratio $\overline{\omega} = \omega/\Omega$, the following dimensionless stiffness ($\overline{K}_{\varepsilon\varepsilon}$, $\overline{K}_{\varphi\varepsilon}$) and damping ($\overline{B}_{\varepsilon\varepsilon}$, $\overline{B}_{\varphi\varepsilon}$) coefficients can be deduced

$$\begin{cases} \overline{K}_{\varepsilon\varepsilon} = -Re\{\overline{W}_{1\varepsilon}\} = \dfrac{K_{\varepsilon\varepsilon}c}{LDP_{s0}} & \overline{K}_{\varphi\varepsilon} = -Re\{\overline{W}_{1\varphi}\} = \dfrac{K_{\varphi\varepsilon}c}{LDP_{s0}} \\ \overline{B}_{\varepsilon\varepsilon} = -\dfrac{Im\{\overline{W}_{1\varepsilon}\}}{\overline{\omega}} = \dfrac{B_{\varepsilon\varepsilon}c\Omega}{LDP_{s0}} & \overline{B}_{\varphi\varepsilon} = -\dfrac{Im\{\overline{W}_{1\varphi}\}}{\overline{\omega}} = \dfrac{B_{\varphi\varepsilon}c\Omega}{LDP_{s0}} \end{cases} \tag{17}$$

Similarly, considering the perturbed film pressure $\varepsilon_0\varphi_1^* e^{i\omega t} P_2$, the restoring forces along ε_0 and φ_0 directions, denoted by $W_{2\varepsilon}$ and $W_{2\varphi}$, respectively, the others resultant stiffness ($\overline{K}_{\varphi\varphi}$, $\overline{K}_{\varepsilon\varphi}$) and damping ($\overline{B}_{\varphi\varphi}$, $\overline{B}_{\varepsilon\varphi}$) coefficients, by using the dimensionless force $\overline{W}_2 = W_2 / LDP_{s0}\varepsilon_0\varphi_1^*$, are given as follows

$$\begin{cases} \overline{K}_{\varepsilon\varphi} = -Re\{\overline{W}_{2\varepsilon}\} = \dfrac{K_{\varepsilon\varphi}c}{LDP_{s0}} & \overline{K}_{\varphi\varphi} = -Re\{\overline{W}_{2\varphi}\} = \dfrac{K_{\varphi\varphi}c}{LDP_{s0}} \\ \overline{B}_{\varepsilon\varphi} = -\dfrac{Im\{\overline{W}_{2\varepsilon}\}}{\overline{\omega}} = \dfrac{B_{\varepsilon\varphi}c\Omega}{LDP_{s0}} & \overline{B}_{\varphi\varphi} = -\dfrac{Im\{\overline{W}_{2\varphi}\}}{\overline{\omega}} = \dfrac{B_{\varphi\varphi}c\Omega}{LDP_{s0}} \end{cases} \tag{18}$$

The bearing stiffness and damping coefficients may be used in rotor dynamic calculations for unbalance and random vibration responses, for determining damped critical speeds and for rotor stability analysis. For these purposes, representing the bearing dynamic coefficients in the *XY* inertial coordinate system is more suitable than in εφ reference system. Equation (19) provides the dynamic coefficients conversion between these two reference coordinate systems.

$$\begin{bmatrix} \overline{K}_{XX} & \overline{K}_{XY} \\ \overline{K}_{YX} & \overline{K}_{YY} \end{bmatrix} = \boldsymbol{T}' \begin{bmatrix} \overline{K}_{\varepsilon\varepsilon} & \overline{K}_{\varepsilon\varphi} \\ \overline{K}_{\varphi\varepsilon} & \overline{K}_{\varphi\varphi} \end{bmatrix} \boldsymbol{T}$$
$$\begin{bmatrix} \overline{B}_{XX} & \overline{B}_{XY} \\ \overline{B}_{YX} & \overline{B}_{YY} \end{bmatrix} = \boldsymbol{T}' \begin{bmatrix} \overline{B}_{\varepsilon\varepsilon} & \overline{B}_{\varepsilon\varphi} \\ \overline{B}_{\varphi\varepsilon} & \overline{B}_{\varphi\varphi} \end{bmatrix} \boldsymbol{T} \tag{19}$$

where, $\boldsymbol{T} = \begin{bmatrix} cos\,\varphi_0 & sin\varphi_0 \\ -sin\varphi_0 & cos\,\varphi_0 \end{bmatrix}$

Numerical Analysis and Results

The bearing and servovalve characteristics adopted in the numerical simulations of the compressor dynamic response are presented in Tab.1.

Table 1. AHJB geometric and operational characteristics adopted for the rotor-bearing simulations.

journal diameter	$D = 100$	*mm*
bearing width	$L = 45$	*mm*
circumferential land width	$a = 9$	*mm*
axial land width	$b = 10$	*mm*
recess depth	$t_r = 1$	*mm*
nominal bearing gap	$c = 90$	μ*m*
constant recess supply pressure range	$P_{s0} = 1.5$ *to* 4.0	*MPa*
servovalve supply pressure	$P_s = 2\,P_{s0}$	*MPa*
lubricant oil dynamic viscosity (*37.8 ℃*)	$\mu = 0{,}015$	Ns/m^2
lubricant oil density	$\rho = 900$	kg/m^3
centered recess pressure ratio	$\beta = 0{,}5$	---
capillary dimensionless parameter	$\delta_c = 17.453$	---
servovalve eigenfrequency	$\omega_v = 2\pi.320$	*rad/s*
servovalve damping factor	$\zeta_v = 0.55$	---
servovalve gain	$K_v = 1x10^{-5}$	$m^3/s/V$
servovalve linear factor	$K_{PQ} = 1.8x10^{-12}$	$Pa/m^3/s$

By applying the shaft and disk finite elements modeling technique proposed by Nelson and McVaugh (1976), the gas compressor shaft is modeled with *56* shaft elements and *57* nodes, as illustrated in Fig.2.

Impellers and other machine elements attached to the shaft are considered as rigid discs, whose dynamics are incorporated into the model by adding inertia to respective nodes. Hence, in the model, the impeller are at nodes *20*, *24*, *28*, *32* and *36*; bushes are at nodes *22*, *26*, *30* and *34*; a thrust disc sleeve is located at node *3*; a balance piston is located at node 38; seal bushes are located are nodes *12* and *46*, and the coupling is at node *55*. The shaft bearings are located at nodes *8* and *50*.

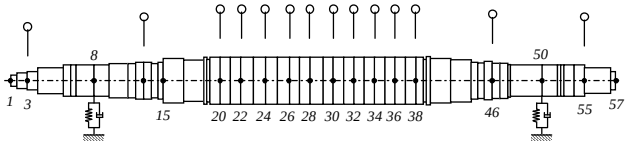

Figure 2. Rotor compressor finite elements model.

The HJB static and dynamic characteristics were extensively investigated by considering different design and operational parameters, characterized by the Sommerfeld number (Watanabe, 2003). Figure 3 shows the journal bearing static dimensionless pressure $\overline{P}_0$ distribution on the land surfaces and recesses due to the static load resulting from half of the compressor weight. The static dimensionless pressures $\overline{P}_{r0}^{(n)}$ in the recesses *1,2,3* and *4* are: *0.3389*, *0.4680*, *0.7194* and *0.4715*, respectively.

The feasibility of influencing the AHJB dynamic fluid film coefficients by the feedback control system gains, aiming at improving the stability of a very simple rotor-bearing system was investigated in Santos and Watanabe (2003). The compensation of the cross-coupling stiffness coefficients and the increase of the direct damping coefficients were proposed in Santos and Watanabe (2004), what leads to rotor-bearing systems with larger threshold of stability. Such results are also used in the present paper.

As mentioned before, the servovalve input signals U_X and U_Y, resulting from the gain and feedback signals combination, have to be in the range of ±5% of the nominal voltage. Besides, bearing dynamic coefficients are only theoretically valid for infinitesimal displacements. However, according to Lund and Thomsen (1978), dynamic coefficients may be used in practical applications for amplitudes up to 50% of the bearing clearance.

Based on these information, the following restrictions of control signal and vibration amplitude were applied to the dynamic coefficients calculations: assuming that the servovalve nominal input signal range is $U_{X,Y}$=±*10V*, the linear actuating signals amplitudes $U^*_{X,Y}$ were restricted to ±*0.25V* range, and the dynamic displacements amplitudes e^* in 20% of nominal bearing gap, i.e., $e^* \le 0.2c$, resulting

$$\begin{cases} \dfrac{U_X^*}{e^*} = (1+k_g)\sqrt{g_{1X}^2 + \omega^2 g_{2X}^2} \le \dfrac{0{,}25}{0{,}2c} \\ \dfrac{U_Y^*}{e^*} = (1+k_g)\sqrt{g_{1Y}^2 + \omega^2 g_{2Y}^2} \le \dfrac{0{,}25}{0{,}2c} \end{cases} \tag{20}$$

The influence of the feedback control gains in the bearing dynamic coefficients is investigated considering synchronous perturbation frequency due to rotor unbalance. Moreover, it is assumed that $g_1 = g_{1X} = g_{1Y}$ and $g_2 = g_{2X} = g_{2Y}$, and k_g, g_1 and g_2 gains are individually varied. It was observed that due to servovalve working limitations, the retrofit of velocity signals in high frequencies rapidly leads to the saturation of servovalve dynamics. Thus, only the proportional gain $g_1 = g_{1X} = g_{1Y}$ will be varied. Assuming that g_2 =*0* and k_g =*2*, the dynamic coefficients of the AHJB were determined as a function of the gain g_1 and the rotation frequency f_r for different values of supply pressure P_{s0}.

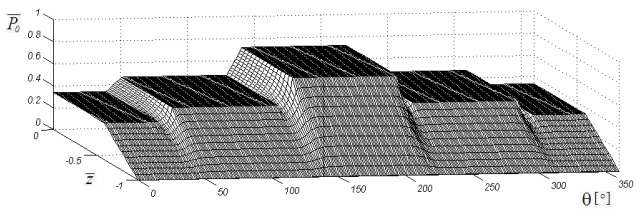

Figure 3. HJB dimensionless static pressure $\overline{P}_0$ distribution, for ε_0 = 0.25 and Λ=2.

Fig.4 to Fig.7 illustrate the stiffness and damping coefficients behavior of the AHJB for P_{s0} =*1.5* and *3.0MPa*. One can clearly notice the influence of rotation frequency and control gain g_1 on the bearing stiffness and damping coefficients. For a given rotation frequency f_r, and varying the control gain g_1, may be noticed three different regions in all figures: two of these regions at the extremities of gain axis g_1 present constant values of the bearing dynamic coefficients and indicate the saturation of the servovalve dynamics. The third region is located in the middle of the gain axis and illustrates the variation of the dynamic coefficients as a function of the gain g_1. For a given frequency f_r such variation can nearly be described by a linear function.

Comparing Figs. 4 and 5 with Figs. 6 and 7, respectively, it can be noticed that the inclination of such linear function is strongly dependent on the supply pressure P_{s0}. Simulation results show that the higher the supply pressure P_{s0} is, the more inclined such a linear behavior is, indicating the feasibility of obtaining large changes of the dynamic coefficients with the increase of P_{s0}. With the increase of rotation frequency f_r such inclination reduces and the curve becomes more flat, indicating the impossibility of achieving significant changes of the dynamics coefficients in high frequencies due to the limitation of the servovalve dynamic response. Summarizing, if large changes of the bearing coefficients are desired and a saturation of the servovalve dynamics is achieved due the amplitude of the control signal, an optional solution is to increase the supply pressure P_{s0}. Moreover, if the bearing coefficients shall be changed in high frequencies, higher response servovalve shall also be used.

Bearing dynamic coefficients, like those presented in Fig.4 to Fig.7, may be used in the gas compressor finite element model to analyze the rotor dynamic behavior. The rotor unbalance response and the damping ratio ζ associated to the first two bending modes are analyzed in the case of bearing hybrid lubrication regime (HJB - $g_1 = g_2$ =0) and the active lubrication regime (AHJB), assuming g_2 =*0*, g_1 =*9x10*^{3}*V/m* and k_g =2. The criteria for choosing a suitable value for control gain g_1 is based on the increasing of damping factor of the first two bending modes of the rotor in *X* and *Y* directions. It is worth to mention that such values were carefully chosen without destabilizing the higher bending mode shapes.

Fig.8 illustrates the behavior of the damping ratio ζ of the first two rotor bending modes, as a function of the rotation frequency, for two different values of the bearing supply pressure P_{s0} (*1.5* and *4.0MPa*) when the bearing operates in the passive (HJB) or active (AHJB) lubrication modes. By analyzing these two graphics, one can notice a significant reduction of the damping ratio ζ as a function of the increase of the rotation frequency f_r and of the supply pressure P_{s0}.

The increase of the rotation frequency leads to instability problems when ζ<0. In the case of instability the gas compressor will vibrate according to its first bending mode shape. For P_{s0} =*1.5MPa*, the instability will occur at the rotation frequency of *131Hz* in the case of HJB and of *151Hz* in the case of AHJB. This shows that the active lubrication, aided by a simple proportional controller with cross-coupling retrofit, can enlarge the stable operational range of the gas compressor. The same behavior can be noticed in case of higher supply pressures. In case of P_{s0} =*4.0MPa*, the instability will occur at the rotation frequency of *158Hz* in the case of HJB and of *177Hz* in the case of AHJB.

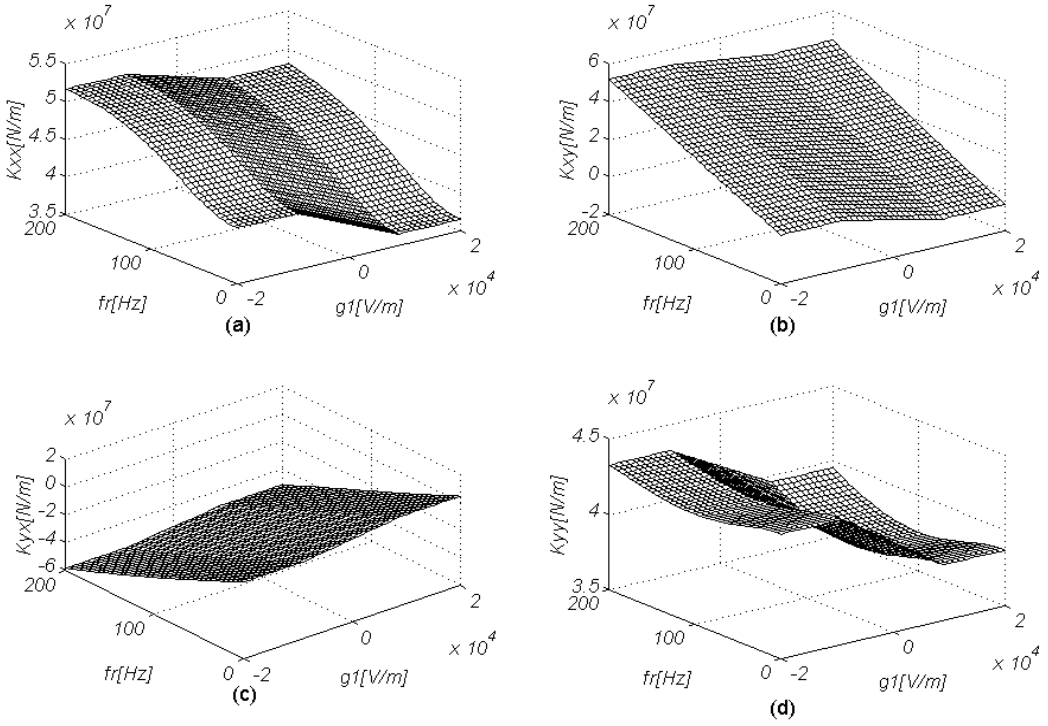

Figure 4. Bearing stiffness coefficients as function of rotation frequency f_r and proportional gain g_1, for P_{s0} =1.5MPa.

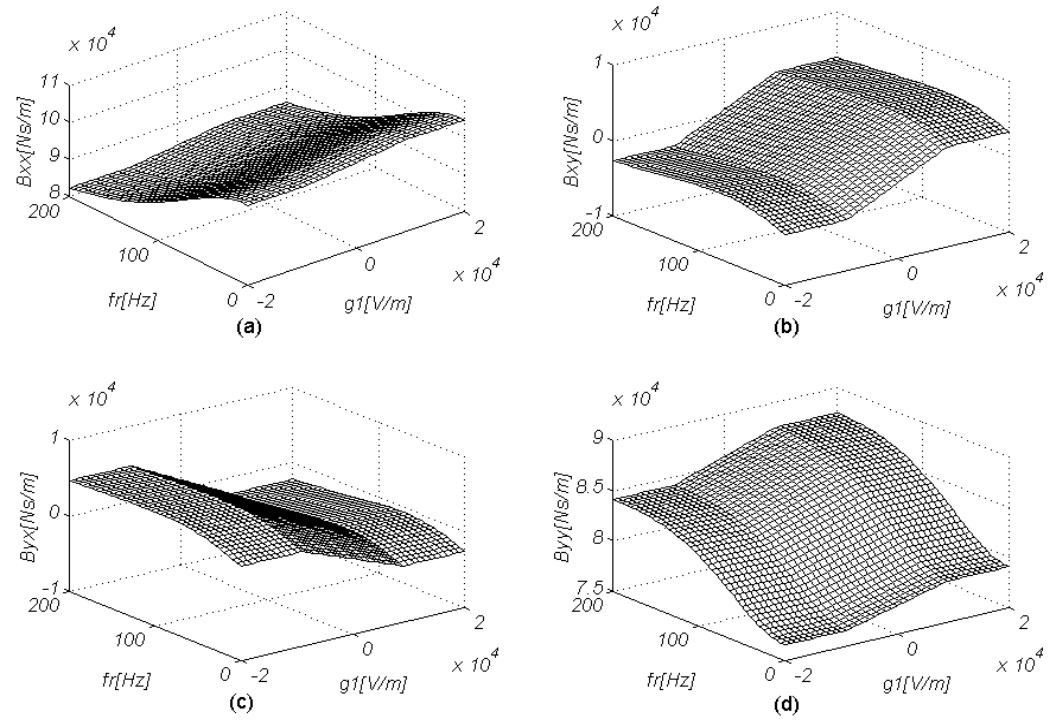

Figure 5. Bearing damping coefficients as function of rotation frequency f_r and proportional gain g_1, for P_{s0} =1.5MPa.

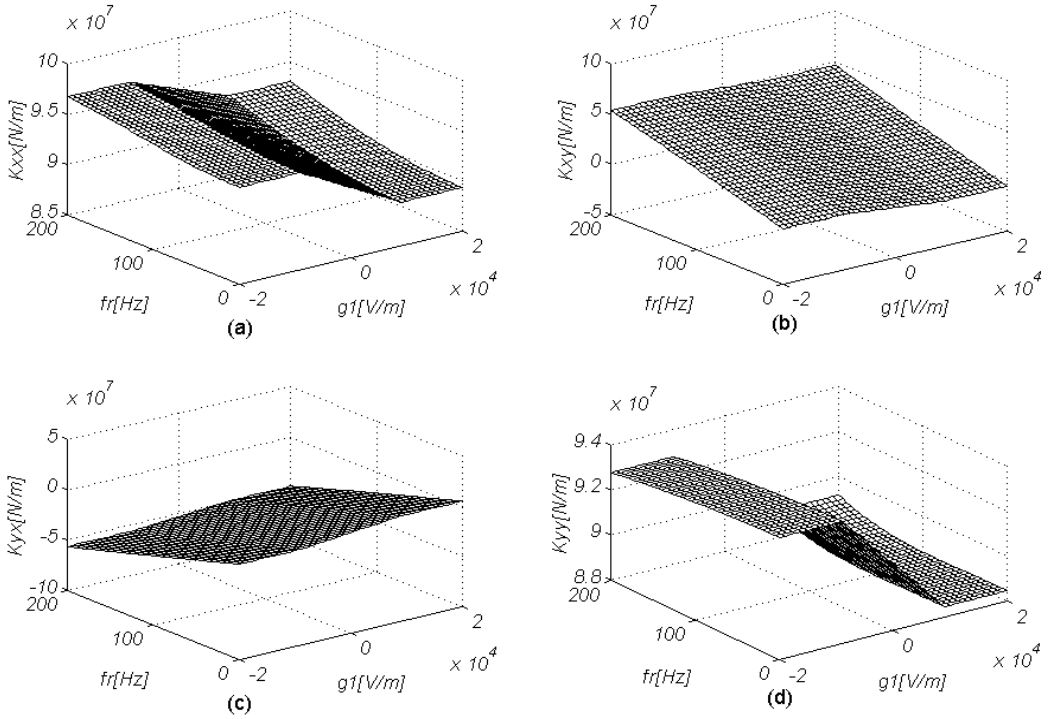

Figure 6. Bearing stiffness coefficients as function of rotation frequency f_r and proportional gain g_1, for P_{s0} =3.0MPa..

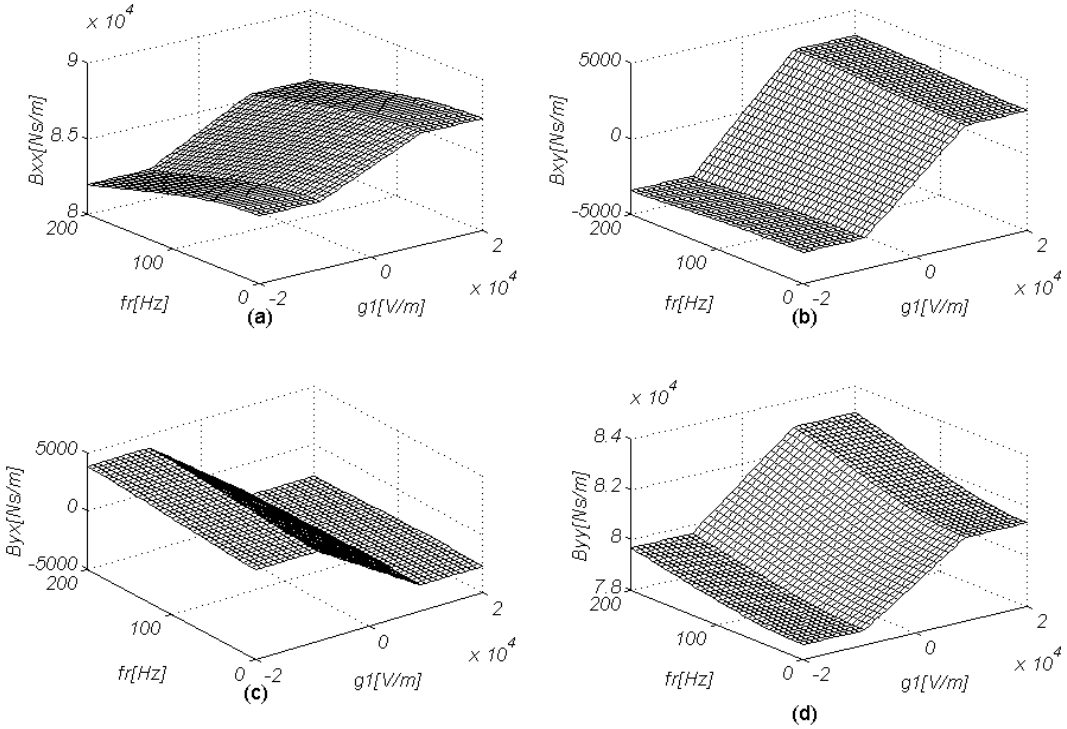

Figure 7. Bearing damping coefficients as function of rotation frequency f_r and proportional gain g_1, for P_{s0} =3.0MPa.

Nevertheless, it is important to point out that, in the special case of multirecess bearings, an increase of the supply pressure will necessarily lead to a simultaneous increase of the stiffness coefficients of the bearing. By increasing the stiffness of the bearings at the nodes *8* and *50*, only small relative movements between compressor shaft and bearing housing will be possible in such nodes. This will deteriorate the capability of dissipation of vibration energy via squeezing the oil film in the bearings. The

consequence is a reduction of the damping ratio ζ in the case of high supply pressures. Moreover, by increasing the supply pressure from *1.5MPa* to *4.0MPa* the difference between the main coefficients in the horizontal and vertical directions become less significant. Such effect can be easily seen comparing the values of ζ in both graphics in the range of low frequencies f_r. Finally, one can claim that the values of damping ratio are reduced at low rotation frequencies by increasing the supply pressure, but the threshold of stability is increased, although the stability reserve is very low (values of ζ very close to zero).

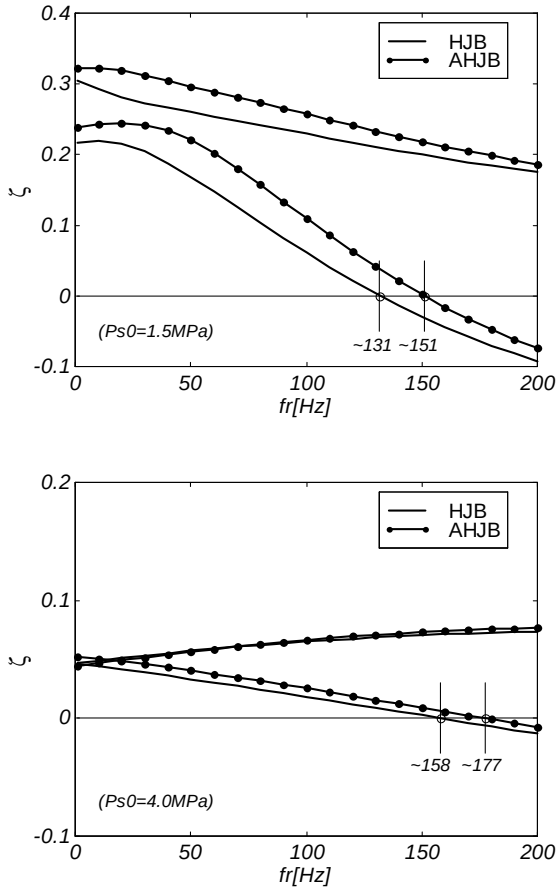

Figure 8. Damping ratio ζ associated to the first two bending mode shapes in the case of gas compressor supported by HJB and AHJB, operating with two different supply pressures: P_{s0} =1.5 and 4.0MPa.

Applying the criteria established by the norm API 617 (1995), one can analyze the rotor unbalance response. According to this norm, for the case in study, the unbalance value to be applied in the node of maximum displacement of the model is given by m_u=*720g.mm*. According to this same norm, the vibration amplitude limit for the case in study is L_v=*16.65μm*. The unbalance response of node *28* (largest amplitude) in X and Y directions is illustrated in Fig.9 in case of hybrid operation with different values of supply pressure P_{s0}. One can notice that, for low values of P_{s0} (*1.5* or *2.0MPa*), the unbalance responses of the compressor are in accordance with API limit, even at critical speed, but for higher values of P_{s0} (*3.0* or *4.0MPa*) the unbalance response of the compressor at critical speeds are higher them the API limit. As mentioned before, in the special case of multirecess journal bearings, an increase of the supply pressure will necessarily lead to a simultaneous increase of the stiffness coefficients of the bearing. By increasing the stiffness of the bearings at the nodes 8 and 50, only small relative movements between compressor shaft and bearing housing will be possible in such nodes. This will deteriorate the capability of dissipation of vibration energy by squeezing the oil film in the bearings and will reduce the damping ratio. Such a claim can be clearly seen in Fig.9.

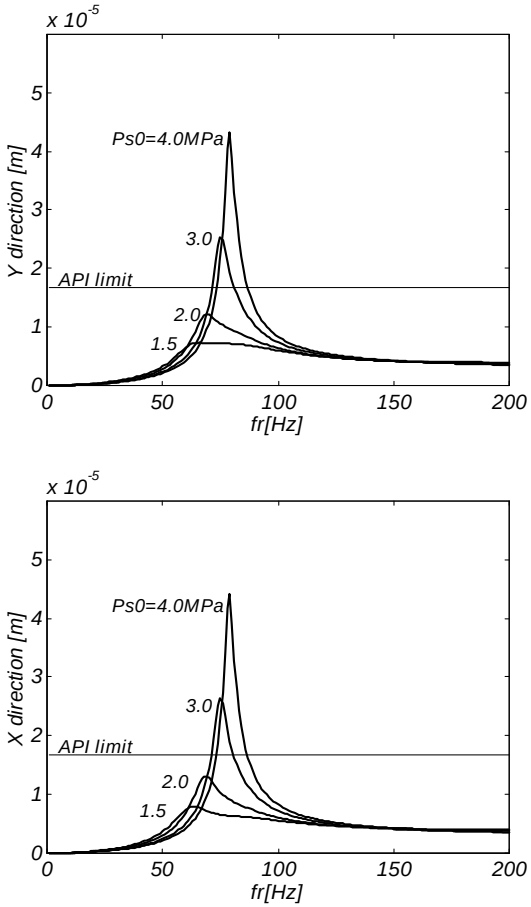

Figure 9. Unbalance response of node 28, in Y and X directions, of the compressor supported by HJB for P_{s0} =1.5; 2.0; 3.0 or 4.0MPa.

From the viewpoint of active lubrication applied to multirecess journal bearings with the aim of controlling lateral dynamics of flexible rotors a paradigm is reached: a) for improving the performance of the active lubrication in such special kind of bearings high values of supply pressure P_{s0} are needed, once the saturation of control signals retrofitted to the servovalves limits the range in which the bearing dynamics coefficients can be modified. Nevertheless, by increasing the supply pressure the main stiffness coefficients of the bearing will also increase; b) for reducing lateral vibrations of the flexible gas compressor it is very important to allow relative large amplitudes of vibration in the bearings, in order to increase the dissipation of vibration energy by squeezing the oil film. It means that it is important to keep low values of main stiffness coefficients, what coerces into working with low values of supply pressure. Fig. 8 presents the comparison of the passive (HJB) and active (AHJB) lubrication modes in the rotor unbalance response for an intermediate value of the supply pressure P_{s0}

(*2.5MPa*), in *X* and *Y* directions, and for both, the API limit is obeyed only with the active lubrication mode. Nevertheless the improvement in reducing the unbalance response is not extraordinary significant, because the supply pressure used is relatively low. Moreover, comparing Fig.9 and Fig.10 one can conclude that a significant reduction of the unbalance response of node *28* can easily be achieved by operating in the (passive) hybrid lubrication mode with low supply pressures in the order of *1.5* and *2.0MPa*.

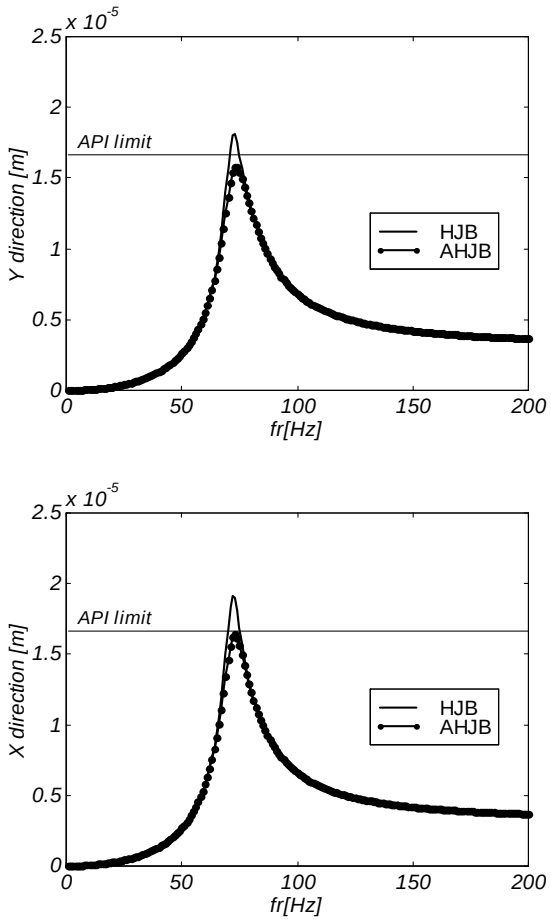

Figure 10. Unbalance response of node 28, in Y and X directions, of the compressor supported by HJB and AHJB, for P_{s0} =2.5MPa.

Conclusions

The mathematical modeling for calculating the static and dynamic characteristics of hybrid multirecess journal bearings, under hybrid and active lubrication regimes, was presented. The feasibility of influencing the oil film dynamic coefficients of such a kind of bearing by means of the servo control system was theoretically illustrated. The feasibility of controlling lateral dynamics of a flexible gas compressor and enlarging its stable operational range were investigated. The active lubrication, aided by a simple proportional controller with cross-coupling retrofit, can enlarge the stable operation range of the gas compressor. In case of supply pressure of P_{s0} *=1.5MPa* it is possible to shift the threshold of instability in approx. 15%, from *131Hz* to *151Hz*. In case of P_{s0} *=4.0MPa*, it is possible to shift the threshold of instability in approx. 12%, from *158Hz* to *177* Hz. Once the stiffness coefficients are strongly influenced by the bearing supply pressure P_{s0}, a suitable choice of the control gains is necessary to comply with the design requirements, unbalance response limits and threshold of instability.

Nevertheless, it is important to point out that, in the special case of multirecess journal bearings, an increase of the supply pressure will necessarily lead to simultaneous increase of the main stiffness coefficients of the bearing. By increasing the stiffness of the bearings, only small relative movements between shaft and bearing housing will be possible. This will deteriorate the capability of dissipation of vibration energy by squeezing the oil film in the bearings and will reduce the damping ratio associated to the first bending mode of the gas compressor. Moreover, a more significant and sufficient improvement of the rotor unbalance response can be achieved by only changing the supply pressure and operating the HJB in its passive form. It is not necessary to operate the bearing in the active form.

In contrast to multirecess journal bearings, tilting-pad journal bearings allow a reduction of the main stiffness of the bearing when the supply pressure is increased due to the tilt movement of the pads, Santos et al. (2004). Thus, the application of active lubrication to tilting-pad journal bearings becomes more efficient than the application to multirecess journal bearings. The reduction of the main stiffness coefficients by increasing the supply pressure allows an optimal improvement of lateral dynamics of flexible rotating shaft via active lubricated tilting-pad bearings.

References

Althaus, J., Stelter, P. Feldkamp, B. and Adam, H., 1993, "Aktives hydraulisches Lager für eine Schneckenzentrifuge, Schwingungen in rotierenden Machinen II", edited by H. Irretirer, R. Nordmann, H. Springer, Vieweg Verlag, Vol.2, pp.28-36. (in German)

API 617 – "Centrifugal Compressors for Petroleum, Chemical, and Gas Service Industries", 1995, 6th ed., American Petroleum Institute.

Bently. D.E., Grant, J.W. and Hanifan, P.C., 2000, "Active Controlled Hydrostatic Bearings for a New Generation of Machines", ASME/IGTI International Gas Turbine & Aeroengine Congress & Exhibition, Munich, Germany, may 8-11, Paper 2000-GT-354.

Edelmann, H., 1986, "Schnelle Proportionalventile und ihre Anwendug, Sonderdruck aus Ölhydraulic und Pneumatik", Vol.30, No.1. (in German)

El-Shafei, A. and Hathout, J.P. 1995, "Development and Control of HSFDs for Active Control of Rotor-Bearing Systems", *ASME Journal of Eng. for Gas Turbine and Power*, Vol.117, No.4, pp.757-766.

Ghosh, M.K., Guha, S.K. and Majumdar, B.C. 1989, "Rotor-Dynamic Coefficients of Multirecess Hybrid Bearings – Part I", *Wear*, Vol.129, pp.245-259.

Goodwin, M.J., Boroomand, T., and Hooke, C.J. 1989, "Variable Impedance Hydrodynamic Journal Bearings for Controlling Flexible Rotor Vibrations", 12th Biennial ASME Conference on Vibration and Noise, Montreal, Sept.17-21, pp.261-267.

Guha, S.K., Ghosh, M.K. and Majumdar, B.C. 1989, "Rotor-Dynamic Coefficients of Multirecess Hybrid Bearings – Part II: Fluid Inertia Effect", *Wear*,Vol. 129, pp.261-272.

Lund, J.W. and Thomsen, K.K., 1978, "A Calculation Method and Data for the Dynamic Coefficients of Oil-Lubricated Journal Bearings, in : Topics in Fluid Film Bearing and Rotor Bearing System Design and Opmization", ASME, New York, pp.1-28.

Merrit, H. E., 1967, "Hydraulic Control System", John Wiley & Sons.

Neal, T.P. 1974, "Performance Estimation for Electrohydraulic Control Systems", Moog Technical Bulletin 126.

Nelson, H.D. and McVaugh, J. M. 1976, "The Dynamics of Rotor-Bearing Systems Using Finite Element", *ASME Journal of Engineering for Industry*, Vol.98, No.2, pp.593-600.

Osman, T.A., Nada, G. S. and Safar, Z. S. 2001, "Static and Dynamic Characteristics of Magnetized Journal Bearings Lubricated with Ferrofluid", *Tribology International*, Vol.34, No.6, pp.369-380.

San Andrés, L. and Lubell, D. 1998, "Imbalance Response of a Test Rotor Supported on Squeeze Film Dampers", *ASME Journal of Engineering for Gas Turbines an Power*, Vol.120, No.2, pp.397-404.

Santos, I.F., 1994, "Design and Evaluation of Two Types of Active Tilting-Pad Journal Bearings", IUTAM Symposium on Active Control of Vibration, Bath, England, pp.79-87.

Santos, I.F. 1995, "On the Adjusting of the Dynamic Coefficients of Tilting-Pad Journal Bearings", *STLE Tribology Transactions*, Vol.38, No.3, pp.700-706.

Santos, I.F. and Nicoletti, R. 1999, "THD Analysis in Tilting-Pad Journal Bearings using Multiple Orifice Hybrid Lubrication, ASME Trans., Journal of Tribology, Vol.121, No.4, pp.892-900.

Santos, I.F. and Nicoletti, R. 2001, "Influence of Orifice Distribution on Thermal and Static Properties of Hybridly Lubricated Bearings", International Journal of Solids and Structures, Vol.38, No.10-13, pp.2069-2081.

Santos, I.F., Nicoletti, R. and Scalabrin, A. 2004, "Feasibility of Applying Active Lubrication to Reduce Vibration in Industrial Compressors", ASME Trans., Journal of Engineering for Gas Turbine and Power, Vol. 126, 4, pp.888-894.

Santos, I.F. and Russo, F.H. 1998, "Tilting-Pad Journal Bearings with Electronic Radial Oil Injection", *ASME Journal of Tribology*, Vol.120, No.3, pp.583-594.

Santos, I.F., and Scalabrin, A. 2003, "Control System Design for Active Lubrication with Theoretical and Experimental Examples", *ASME Journal of Engineering for Gas Turbine and Power*, Vol.125, 1, pp.75-80.

Santos, I.F., Scalabrin, A. and Nicoletti, R. 2001, "Ein Beitrag zur aktiven Schmierungstheorie, Schwingungen in Rotierrenden Machinen VI", edited by H. Irretier, R. Nordmann, H. Springer, Vieweg Verlag, Vol.5, pp.21-30. (in German)

Santos, I.F. and Watanabe, F.Y., 2003, "Feasibility of Influencing the Dynamic Fluid Film Coefficients of a Multirecess Journal Bearing by Means of Active Hybrid Lubrication", *RBCM – Journal of the Brazilian Society of Mechanical Sciences*, Vol. 25, No. 2, pp.154-163.

Santos, I.F. and Watanabe, F.Y., 2004, "Compensation of Cross-Coupling Stiffness and Increase of Direct Damping in Multirecess Journal Bearings using Active Hybrid Lubrication – Part I: Theory", *ASME Journal of Trybology*, Vol. 126, pp.146-155.

Ulbrich, H. and Althaus, J. 1989, "Actuator Design for Rotor Control", 12th Biennial ASME Conference on Vibration and Noise, Montreal, Sept.17-21, pp.17-22.

Vance, J.M. and Li, J. 1996, "Test Results of a New Damper Seal for Vibration Reduction in Turbomachinery", *ASME Journal of Engineering for Gas Turbines and Power*, Vol.118, No.4, pp.843-846.

Watanabe, F.Y., 2003, "Active Lubrication Applyied to Hybrid Journal Bearings", PhD Thesis, Unicamp, 169p. (in Portuguese).